

Effect of correlation on the properties of 2D spin-polarized dipolar Fermi gas

Rashmi Gangwar¹ , Arup Banerjee^{1,2} and Amit Das³

¹Human Resources Development section, Raja Ramanna Centre for Advanced Technology, Indore 452013, India

²Homi Bhabha National Institute, Training School Complex, Anushaktinagar, Mumbai 400094, India

³Laser Materials Processing Division, Raja Ramanna Centre for Advanced Technology, Indore 452013, India

E-mail: rashmigangwar17@gmail.com

Received 19 July 2019, revised 17 November 2019

Accepted for publication 6 December 2019

Published 10 January 2020



CrossMark

Abstract

The spin-polarized 2D dipolar Fermi gas trapped in a harmonic potential provides an opportunity to study the many-fermion systems with strong particle–particle correlation in a controlled fashion. In this paper, we investigate the role of the correlation part of the interaction energy on the ground-state properties and on the collective oscillation frequencies of a 2D dipolar Fermi gas by employing density functional theory (DFT) within local density approximation. We employ a purely density-based, orbital-free approach of DFT to study the ground-state properties. We employ an orbital-free approach, as it is suitable for handling a large number of fermions (10^3 – 10^4 atoms/molecules), which are typically the number of atoms/molecules contained in the samples of dipolar Fermi gas created in the laboratories. We derive analytical expressions for the frequencies of the monopole and quadrupole modes of the collective oscillations by employing a method based on the sum-rule approach of linear response theory. We find that the exchange and correlation part of the fermion–fermion interaction contributes significantly to the total energy, and their contributions increase with increasing number of fermions and interaction strength. In particular, the correlation part lowers the total energy of the 2D dipolar fermionic system, thereby stabilizing the system. Similarly, the inclusion of the correlation effect lowers the frequencies of the monopole mode of the collective oscillations appreciably in comparison to the case when this effect is not taken into account. On the other hand, the frequency of the quadrupole mode of the collective oscillations is not appreciably altered by the correlation part of the interaction over a wide range of values of interaction strength and number of fermions.

Keywords: dipolar Fermi gas, density functional theory, collective oscillations

(Some figures may appear in colour only in the online journal)

1. Introduction

The many-body system of ultracold dipolar Fermi gas grabbed the attention of the research community because of the unique and long-range anisotropic nature of the interaction between the dipolar atoms or molecules [1]. Experimental realization of degenerate dipolar gas of fermionic atoms or molecules such as $^{40}\text{K}^{87}\text{Rb}$ and $^{23}\text{Na}^{40}\text{K}$ [2–7] opened the door to understanding the many-body physics associated with the correlated fermionic system. The novel physics of both the equilibrium and dynamical properties of such systems can

be explored as functions of the strength and type (attractive or repulsive) of interaction, geometry of the trapping potential and the dimensionality of the system. The long-range anisotropic nature of the interaction potential is expected to yield interesting physical properties such as topological superfluidity with fermionic molecules [8–10], interlayer pairing between 2D systems [11, 12] and the formation of dipolar quantum crystals [13].

The dipolar Fermi gases confined in a 2D trapping potential are of particular interest as the strong suppression in reaction rate for a gas of hetero-molecules in a 2D geometry

results in enhancement of the lifetime of molecules, thereby stabilizing the dipolar Fermi gas [6]. The 2D dipolar Fermi gases have been realized experimentally by tight trapping along one (mostly vertical) direction [14–18]. These 2D dipolar Fermi gases provide scope for studying the fermionic system with strong correlations. For example, in a series of recent theoretical studies it has been shown that 2D Fermi gas can undergo interesting quantum phase transition from a normal Fermi liquid-like state at low densities to a more ordered 1D strip phase (1DSP) for lower dipolar strength or a triangular Wigner crystal phase for higher dipolar strength [19]. Due to the interesting properties of 2D Fermi gases, the ground-state properties of both uniform and harmonically trapped 2D dipolar fermions have been calculated by employing theoretical methods based on Hartree–Fock formalism and density functional theory (DFT) [19–29]. In this paper, we employ a DFT-based approach to calculate the ground-state properties of a spin-polarized dipolar Fermi gas trapped in a 2D harmonic oscillator potential. We employ the DFT-based method for two reasons: (1) DFT takes into account the effect of both exchange and correlation arising from the Pauli exclusion principle and inter-fermion interaction and (2) DFT is suitable for handling fermionic systems with a large number of particles, as the basic variable of this formalism is particle density—a function of just three spatial variables [30–32]. In principle, DFT is exact in nature. However, due to a lack of knowledge of the exact forms of the exchange and correlation functional, it becomes necessary to use approximate forms for them to carry out any practical calculation. For electronic systems, a tremendous amount of effort has gone into the development of exchange and correlation functionals with increasing degree of accuracy [31, 32]. Recently, approximate expressions for both exchange (Hartree and exchange together) and correlation energy functionals for a spin-polarized 2D dipolar Fermi gas have been derived within local density approximation (LDA) by replacing the constant particle density in the expressions for exchange and correlation energies of a corresponding homogeneous gas by the local density of the inhomogeneous system [23, 24]. In a very recent study, the accuracy of these LDA-based expressions for exchange and correlation functionals have also been assessed against the exact results for a model system of two dipolar fermions [33]. It has been found that the exchange and correlation energies are a sizeable part of the total energy and their contributions increase with higher value of interaction strength.

In this paper, our main aim is to study the effect of the exchange and correlation parts of the interaction between the dipolar fermions on the ground-state properties and collective oscillations of a harmonically trapped 2D dipolar Fermi gas. In view of the large number of fermions (typically N of the order of 10^3 – 10^4), we employ an orbital-free DFT (OF-DFT)-based approach rather than the orbital-based Kohn–Sham approach of DFT. For such systems with a large number of particles, the purely density-based OF-DFT approach is more advantageous as it scales approximately linearly with particle number N in contrast to the N^3 scaling of the orbital-based Kohn–Sham approach. Consequently, the calculations of

ground-state properties of 2D dipolar fermions by the OF-DFT-based approach can be accomplished with significantly less computational cost and effort. We note here that the OF-DFT-based approach has been employed previously to study the ground-state properties of 2D dipolar Fermi gas within Thomas–Fermi (TF) [23] and Thomas–Fermi–von Weizsacker (TFvW) [24] models including only the effect of exchange and completely ignoring the effect of fermion–fermion correlation. To calculate the frequency of the collective oscillations, we use the sum-rule-based approach [34, 35] and derive analytical expressions for frequencies of the monopole and quadrupole modes of collective oscillations. The calculation of these frequencies requires ground-state densities of the system as input, which are obtained by employing the OF-DFT-based approach.

In section 2, we present a brief derivation of the Kohn–Sham-like equation in terms of the density of fermions within the OF-DFT-based approach. In section 3, we present and discuss the results. The paper is concluded in section 4.

2. Methodology

2.1. OF-DFT for ground-state properties

We consider a system of N identical spin-polarized fermionic neutral atoms (or molecules) of mass m with electric dipole moment d , which are polarized along the z axis and confined in the x - y plane by a 2D isotropic harmonic oscillator potential having radial trap frequency ω . These fermions interact with each other via an isotropic repulsive potential given by,

$$v_{dd}(\mathbf{r}) = \frac{C_{dd}}{r^3}, \quad (1)$$

where r is the distance between the dipoles and $C_{dd} = d^2/4\pi\epsilon_0$ denotes the strength of dipolar interaction. To calculate the ground-state properties of the above-mentioned 2D dipolar Fermi gas, we use the OF-DFT-based method, which takes into account the effect of both exchange and correlation within LDA. In accordance with the basic theorem of DFT, the ground-state energy of a collection of N dipolar fermions can be written as a functional of the single-particle density $\rho(\mathbf{r})$ [30, 32]:

$$E[\rho] = T_s[\rho] + \int v_{ext}(\mathbf{r})\rho(\mathbf{r})d\mathbf{r} + E_{int}[\rho], \quad (2)$$

where $T_s[\rho]$ denotes the kinetic energy of a non-interacting N -particle system in a multiplicative potential, the state of the system is represented by a Slater determinant constructed from the lowest energy solutions of the Schrödinger equation, and it is determined by the expectation value of the kinetic energy operator in this state. On the other hand, the interacting kinetic energy $T[\rho]$ is determined by the expectation value of the kinetic energy operator in the exact many-body state and its magnitude is higher than that of $T_s[\rho]$. The term $E_{int}[\rho]$ in the above expression represents the interaction energy functional, which takes into account the effects of both classical and quantum mechanical many-body interactions.

We note here that $E_{int}[\rho]$ also includes a contribution of small difference $T[\rho] - T_s[\rho]$, which is introduced due to the replacement of the interacting kinetic energy functional by a non-interacting one. The major contribution to the quantum part of $E_{int}[\rho]$ comprises the exchange and correlation energy functionals capturing the effect of the Pauli exclusion principle and fermion–fermion correlation in the many-body wave function, respectively. The second term in the above equation represents the energy due to the interaction of N fermions with the external 2D harmonic trapping potential $v_{ext}(\mathbf{r})$ ($=\frac{1}{2}m\omega^2r^2$), which is used for confining these fermions.

For non-interacting kinetic energy functional $T_s[\rho]$, we make use of the expression proposed and tested in [24] within TFvW approximation given by,

$$T_s[\rho] = T_{TF}[\rho] + T_{vW}[\rho], \quad (3)$$

with

$$T_{TF}[\rho] = \frac{\pi\hbar^2}{m} \int \rho(\mathbf{r})^2 d\mathbf{r}, \quad (4)$$

and

$$T_{vW}[\rho] = \lambda_{vW} \frac{\hbar^2}{8m} \frac{1}{8} \int \frac{|\nabla\rho(\mathbf{r})|^2}{\rho(\mathbf{r})} d\mathbf{r}. \quad (5)$$

In the above equations, $T_{TF}[\rho]$ corresponds to the kinetic energy functional of a fermionic system in 2D within LDA and $T_{vW}[\rho]$ denotes the von Weizsacker correction to the kinetic energy functional originating from the inhomogeneity in the density. We note here that for the 2D case conventional methods do not yield any gradient correction and therefore to incorporate the effect of inhomogeneity, in analogy with the 3D case a gradient-dependent von Weizsacker-like term has been introduced with λ_{vW} as a parameter. It has been shown in [24] that the parameter λ_{vW} depends weakly upon the number of particles in the system and is related to N by $\lambda_{vW} = \lambda_{vW}^\infty + p/N^q$ with $\lambda_{vW}^\infty = 0.0184$, $p = 0.0577$ and $q = 0.1572$.

Next, following general convention of DFT, we divide $E_{int}[\rho]$ into two parts:

$$E_{int}[\rho] = E_{HF}[\rho] + E_c[\rho], \quad (6)$$

where $E_{HF}[\rho]$ is analogous to the Hartree–Fock (HF) energy, which is a sum of two terms, one taking into account the effect of classical dipole–dipole interaction (Hartree energy) and the other one accounts for exchange interaction. On the other hand, $E_c[\rho]$ denotes the correlation energy arising from the quantum mechanical inter-particle correlations. It is important to note that even for 2D uniform dipolar Fermi gas, individually both Hartree and exchange energies are singular due to $1/r^3$ form of the interaction potential. However, the singularities in Hartree and exchange energies get canceled when the two energies are evaluated with appropriate regularization of the dipole–dipole interaction potential $v_{dd}(\mathbf{r})$. To calculate the energies it is required that the regularized potential should not have singularity at $r = 0$. This is achieved by associating with each interacting physical electrical dipole a Gaussian charge distribution [23, 24]. Upon

regularization, the HF part E_{HF} can be decomposed as,

$$E_{HF}[\rho] = E_{HF}^1[\rho] + E_{HF}^2[\rho], \quad (7)$$

with

$$E_{HF}^1[\rho] = a_{dd} \frac{\hbar^2}{m} \int \frac{256}{45} \sqrt{\pi} \rho(r)^{5/2} d\mathbf{r}, \quad (8)$$

$$E_{HF}^2[\rho] = -\frac{\pi\hbar^2 a_{dd}}{m} \int \rho(\mathbf{r}) d\mathbf{r} \int d\mathbf{r}' \int \frac{d\mathbf{k}}{(2\pi)^2} k e^{-i\mathbf{k}\cdot(\mathbf{r}-\mathbf{r}')} \rho(\mathbf{r}'), \quad (9)$$

where $a_{dd} = mC_{dd}/\hbar^2$. We note here that the above expression for $E_{HF}^1[\rho]$ is obtained from the results for uniform dipolar Fermi gas within LDA. On the other hand, the above expression for $E_{HF}^2[\rho]$ is an exact one and it is spatially non-local in nature. This term vanishes for a uniform system. As with $E_{HF}^1[\rho]$, the exact form of the correlation energy $E_c[\rho]$ is not known and one needs to use an approximate expression for it to perform any calculation. To this end, several researchers have derived an expression for correlation energy within LDA by various methods [25]. In this paper, we employ the expression derived in [25] by using an empirical fit to the data obtained through Monte Carlo simulation for uniform gas given by,

$$E_c[\rho] = \int \rho(\mathbf{r}) \epsilon_c(\rho) d\mathbf{r}. \quad (10)$$

ϵ_c being correlation energy per particle, is obtained using an empirical fit to quantum Monte Carlo simulation (QMC) data in [25] as the following,

$$\epsilon_c(\rho) = \frac{-2\pi^2\hbar^2 a_{dd}^2}{m} \rho^2 \ln \left[1 + \frac{1}{A\rho^{1/2} + B\rho + C\rho^{3/2}} \right], \quad (11)$$

where $A = 1.2x_c^{1/4}$, $B = 1.1017x_c^{1/2}$, $C = -0.0100x_c^{3/4}$ with $x_c = (4\pi a_{dd}^2)$. The above parameterized form for the correlation energy functional yields results for total energy, which match well with the corresponding QMC data up to $\lambda_0 = \sqrt{x_c \rho_a} = 72$, where ρ_a is the average density defined as $\rho_a = \frac{\int \rho(\mathbf{r}) d\mathbf{r}}{\int d\mathbf{r}}$.

Having set up the energy functional for a system of spin-polarized dipolar fermions trapped in a 2D harmonic oscillator potential, we now exploit the variational nature of the ground-state energy with respect to the density (second part of the Hohenberg–Kohn theorem) [30] to derive a working equation for calculation of the ground-state density. By making the total energy functional (given in equation (2)) stationary with respect to density $\rho(\mathbf{r})$ along with normalization constraint condition $\int |\rho(\mathbf{r})| d^2\mathbf{r} = N$, we get the following Euler equation:

$$\delta T_s / \delta \rho + v(\mathbf{r}) = \mu, \quad (12)$$

where μ is the chemical potential and $v(\mathbf{r})$ is the effective potential given by,

$$v(\mathbf{r}) = \frac{1}{2} m\omega^2 r^2 + \delta E_{int} / \delta \rho. \quad (13)$$

By defining $\phi(\mathbf{r}) = \sqrt{\rho(\mathbf{r})}$ and $v_{int}(\mathbf{r}) = \delta E_{int} / \delta \rho$, the above Euler equation can be transformed to a Kohn–Sham-like

equation given by,

$$-\frac{\lambda_{vW}}{2} \frac{\hbar^2}{2m} \nabla^2 \phi(r) + v_{\text{eff}}(\mathbf{r}) \phi(\mathbf{r}) = \mu \phi(\mathbf{r}), \quad (14)$$

with

$$v_{\text{eff}}(\mathbf{r}) = \frac{2\pi\hbar^2}{m} \phi^2(\mathbf{r}) + \frac{1}{2} m \omega^2 r^2 + v_{\text{int}}(\mathbf{r}), \quad (15)$$

where $v_{\text{int}}(r)$ is given by,

$$v_{\text{int}}(\mathbf{r}) = v_{\text{HF}}^1(\mathbf{r}) + v_{\text{HF}}^2(\mathbf{r}) + v_c(\mathbf{r}), \quad (16)$$

with

$$\begin{aligned} v_{\text{HF}}^1(\mathbf{r}) &= \frac{128\hbar^2 a_{dd}}{9m} \sqrt{\pi} \rho^{3/2}(\mathbf{r}) \\ v_{\text{HF}}^2(\mathbf{r}) &= \frac{-2\pi\hbar^2 a_{dd}}{m} \int d\mathbf{r}' \int \frac{d\mathbf{k}}{(2\pi)^2} k e^{-i\mathbf{k}\cdot(\mathbf{r}-\mathbf{r}')} \rho(\mathbf{r}') \\ v_c(\mathbf{r}) &= \epsilon_c(\rho) + \rho(\mathbf{r}) \frac{\partial \epsilon_c}{\partial \rho}. \end{aligned} \quad (17)$$

We note that the first term in the Kohn–Sham-like equation, equation (14), arises from the functional derivative of $T_{vW}[\rho]$ and on the other hand, the functional derivative of $T_{\text{TF}}[\rho]$ yields the first term in $v_{\text{eff}}(\mathbf{r})$. By further dividing both sides of equation (14) by λ_{vW} , it can be rewritten as,

$$-\frac{\hbar^2}{2m} \nabla^2 \phi(r) + v'_{\text{eff}} \phi(r) = \mu' \phi(r), \quad (18)$$

where $v'_{\text{eff}} = v_{\text{eff}}/\lambda_{vW}$ and $\mu' = \mu/\lambda_{vW}$.

To obtain the ground-state density $\rho(\mathbf{r})$ ($\phi(\mathbf{r})$), we need to solve the above Kohn–Sham-like equation in which the potential $v'_{\text{eff}}(\mathbf{r})$ itself depends on $\rho(\mathbf{r})$. To solve equation (18), we apply a self-consistent imaginary-time propagation technique, which has previously been used quite successfully for solving the Kohn–Sham-like equation in the realm of electronic systems [36]. A brief description of the self-consistent method, which we employed, is presented in appendix A. In the next section, we present and discuss the results for the ground-state properties of 2D dipolar fermions obtained by solving equation (18). Furthermore, using the ground-state densities, we also calculate the frequencies of the monopole and quadrupole modes of the collective oscillations by employing a method based on the sum-rule approach of linear response theory, and these results are also presented in the next section.

3. Result and discussion

3.1. Ground-state properties

Before proceeding with the discussion on the results we obtained, we make a survey of the basic characteristic parameters of the samples of dipolar Fermi gas, which have been realized experimentally by various groups. Recently, a series of experiments [2, 3] have reported realization of dense gas of 4×10^4 polar molecules of $^{40}\text{K}^{87}\text{Rb}$ at a temperature below 400 nK. The electric dipole moment of KRb molecules is found to be 0.5 D (where $1\text{D} = 3.335 \times 10^{-30}\text{C m}$), yielding

the dipolar strength $a_{dd} \approx 0.47\ \mu\text{m}$. In a very recent experiment, De Marco *et al* [7] have also reported realization of a degenerate gas of 10^5 fermionic $^{40}\text{K}^{87}\text{Rb}$ molecules at 250 nK and another sample at 50 nk containing 2.5×10^4 of the same molecules. In this experiment, the fermionic cloud of KRb molecules is trapped in a harmonic potential with frequency $\omega = 2\pi \times 40\text{ Hz}$, which corresponds to the value of harmonic oscillator length $a_{ho} \approx 1.42 \times 10^{-6}m$ (where $a_{ho} = \sqrt{\hbar/m\omega}$), thereby resulting in dimensionless interaction strength of the order of $a_{dd}/a_{ho} \approx 0.33$. In another experiment, Park *et al* [5] reported realization of ultracold dipolar Fermi gas of 5×10^3 molecules of $^{23}\text{Na}^{40}\text{K}$ in a harmonic trap with frequency $\omega = 2\pi \times 160\text{ Hz}$. The dipole moment of NaK molecule is $d = 0.8\text{D}$, which corresponds to $a_{dd} = 0.6\ \mu\text{m}$ and $a_{dd}/a_{ho} \approx 0.6$.

We carry out theoretical calculations for several values of dipolar strength a_{dd}/a_{ho} and number of dipolar fermions N in accordance with the experimentally realized values, as discussed above. We begin with the discussion of our results, highlighting the effect of inter-particle correlation on the ground-state properties followed by the results for frequencies of the collective oscillations of trapped 2D dipolar Fermi gases. Before proceeding with the detailed discussion of the results, we wish to note here that the ratio $|E_{\text{HF}}^2/E_{\text{HF}}^1|$ scales as $1/\sqrt{N}$ in the large- N limit [23, 24]. Consequently, for $N \gg 1$, the contribution of the non-local term E_{HF}^2 will be significantly lower than that of E_{HF}^1 to the total energy. This has also been verified in [24] by calculating the two energy components using the ground-state densities of a collection of fermions trapped in a harmonic oscillator potential without dipolar interaction. It has been found that with increasing number of fermions N , the value of the above ratio diminishes from around 0.13 for $N = 55$ to 0.013 for $N = 5151$. To study the effect of dipolar interaction on the above ratio, we solve equation (18) for $a_{dd}/a_{ho} = 0.3$ and N is varied from 10^2 to 10^4 . In table 1, we present the results for different energy components along with the total energy and the corresponding ground-state density profiles are displayed in figure 1. It can be clearly seen from table 1 that the ratio $|E_{\text{HF}}^2/E_{\text{HF}}^1|$ decreases from around 0.03 for $N = 10^3$ to 0.01 for $N = 10^4$ in conformity with the $1/\sqrt{N}$ scaling mentioned above. Moreover, we also note that as N is increased from 10^2 to 10^4 , the percentage contribution of the non-local part E_{HF}^2 to the total energy reduces from around 2.48% to 0.40%. Whereas, for the same values of N , the contribution of local term E_{HF}^1 to the total energy increases from around 34% to 41%. Furthermore, it can be seen from figure 1 that for N ranging from 10^3 to 10^4 , the ground-state density profiles with and without the inclusion of non-local terms hardly exhibit any appreciable differences. As we are interested in studying the properties of dipolar fermions with $N \gg 1$, and in view of the results discussed above, we safely ignore the contribution of non-local term E_{HF}^2 and use the approximate expression $E_{\text{HF}} \approx E_{\text{HF}}^1$.

Having appraised the contribution of E_{HF}^2 towards the total energy, we next focus our attention on the role of the correlation energy E_c in determining the ground state and the collective oscillation properties of spin-polarized 2D

Table 1. Results for various ground-state energy components along with the total energy (per particle) as a function of the number of fermions N . The percentage contribution of the exchange energy E_{HF}^1 , non-local energy E_{HF}^2 and the correlation energy E_c to the total energy have been listed in the last three columns. The results for the energies are in the unit of harmonic oscillator energy $\hbar\omega$.

$a_{dd}/a_{ho} = 0.3$								
N	E_{Total}	E_{int}	E_{HF}^1	E_{HF}^2	E_c	$ E_{HF}^1 $ (%)	$ E_{HF}^2 $ (%)	$ E_c $ (%)
100	12.411	2.260	3.250	-0.309	-0.681	26.18	2.48	5.48
1000	44.725	10.938	15.191	-0.469	-3.785	33.96	1.05	8.46
2500	74.781	19.670	27.468	-0.535	-7.263	36.73	0.72	9.71
5000	110.498	30.492	42.920	-0.591	-11.837	38.84	0.53	10.71
7500	138.938	39.335	55.684	-0.626	-15.723	40.07	0.45	11.32
10000	163.501	47.090	66.957	-0.651	-19.216	40.95	0.40	11.75

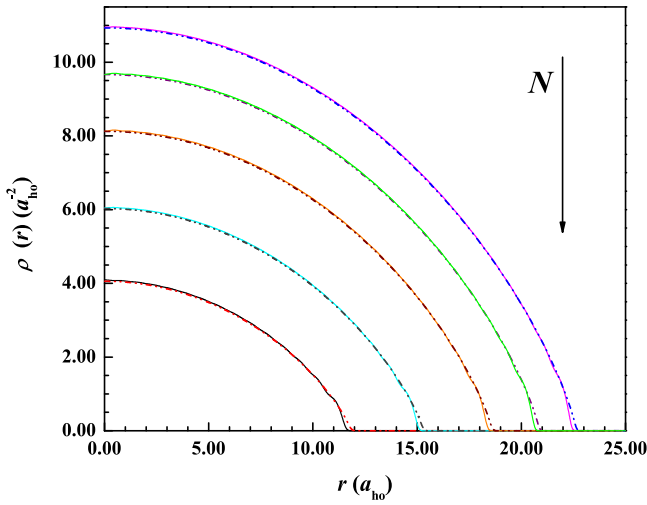


Figure 1. Comparison of the ground-state densities obtained with and without the contribution of the non-local potential E_{HF}^2 (equation (17)) for $a_{dd}/a_{ho} = 0.3$, and for different values of the number of dipolar fermions such as 10 000, 7500, 5000, 2500 and 1000 (order is indicated by a downward arrow). Solid curves correspond to the density with non-local contribution and the dotted curves correspond to the distribution obtained without non-local contribution.

dipolar fermions. We point out here that the range of values of dipolar strength a_{dd}/a_{ho} and the number of fermions N chosen to perform the calculations are consistent with the validity range of LDA-based expression for the correlation energy given by equation (11). For example, for $N = 10^4$ and $a_{dd}/a_{ho} = 1.0$ we get $\lambda_o \approx 7.0$, which is well below the validity limit of $\lambda_o \approx 72$. We note here that the negative values of correlation energy signify that the corresponding potential is attractive in nature and thus helps in lowering the ground-state energy of the system. Moreover, we find that the contribution of correlation energy increases with higher values of N . For example, the contribution of the correlation part of the interaction to the total energy increases from around 8.5% at $N = 10^3$ to about 12% at $N = 10^4$ for dipolar strength $a_{dd}/a_{ho} = 0.3$. Similarly, the ratio $|E_c/E_{HF}^1|$ also increases from around 0.25 for $N = 10^3$ to 0.29 for $N = 10^4$. We note here that unlike the electronic case, for spin-polarized dipolar fermions, the contribution of correlation energy is quite sizeable to the total energy. Consequently, the

LDA-based expression for the interaction energy will over-estimate the total energy of the system if the correlation part is not taken into account.

Next, we focus our attention on the ground-state density profiles of trapped 2D dipolar Fermi gas and how these profiles are affected by the correlation part of the inter-particle interaction. To this end, in figure 2 we compare the ground-state density profiles of dipolar fermions with and without the inclusion of the correlation energy term in the total energy functional for various values of particle number N and dipolar interaction strength a_{dd}/a_{ho} . From this figure, first we note the following general features of the density profiles (see dashed curves in the figure): (a) for a given value of N , the peak density shows a decreasing trend and correspondingly the radius of the cloud increases for stronger dipole interaction, and (b) for a given value of the interaction strength, the size of the density profile increases with increasing value of N . This behavior is attributed to the repulsive nature of 2D dipole-dipole interaction force and the enhancement of this repulsion with increasing number of fermions.

Now, we proceed with the assessment of the effect of correlation on the density distribution of trapped 2D dipolar fermions. To this end, we observe from figure 2 that with the inclusion of the effect of correlation, the maxima of the density profiles is enhanced and the corresponding radius of the cloud is shortened. For example, with the correlation effect included, the radius of the cloud for $a_{dd}/a_{ho} = 0.3$ and $N = 10^4$ decreases by around 6% with respect to the case when correlation is not taken into account. On the other hand, after including the correlation energy term and keeping the other parameters at the same values, the peak of the density profile increases by around 13% over the density profile obtained without the inclusion of the correlation energy term. This indicates that the correlation potential is attractive in nature, which pulls the fermions towards the center, thereby increasing the central density and reducing the radius of the cloud. Furthermore, this modification in the density profiles become more prominent for a larger number of particles and for higher values of dipole-dipole interaction strength.

To further estimate the contribution of the correlation energy term to the total energy and to study its role on the ground-state properties, we estimate the percentage relative difference in the

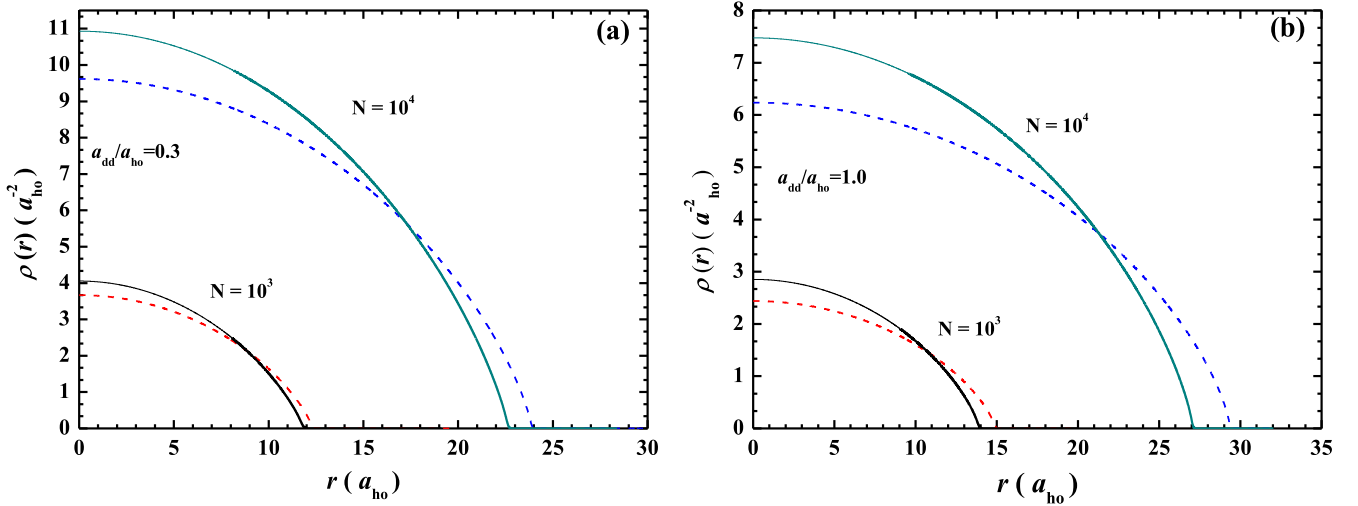


Figure 2. Comparison of the ground-state densities obtained with and without contribution of the correlation part in the inter-fermion interaction energy. Dashed and continuous lines correspond to ground-state densities without and with the correlation term taken into account, respectively: (a) $a_{dd}/a_{ho} = 0.3$, (b) $a_{dd}/a_{ho} = 1.0$. In each figure, the densities are also shown for two different values of the number of particles N ($=10\,000$ and 1000).

Table 2. Comparison of the total ground-state energy (per fermion) obtained without (woc) and with (wc) the contribution of the correlation energy term taken into account for different values of the number of fermions N with $a_{dd}/a_{ho} = 0.3$. The last column presents the results for the percentage relative difference in the total energy ($\Delta E = |E_{Total}^2 - E_{Total}^1|$) as a function of N . The results for the energies are in the unit of harmonic oscillator energy $\hbar\omega$.

$a_{dd}/a_{ho} = 0.3$			
N	E_{Total}^1 (woc)	E_{Total}^2 (wc)	$\Delta E/E_{Total}^2$ (%)
100	13.358	12.715	5.05
1000	48.613	45.185	7.58
2500	81.868	75.309	8.71
5000	121.735	111.083	9.59
7500	153.673	139.558	10.11
10000	181.366	164.148	10.49

total energy $\Delta E/E_{Total}^2$ (where $\Delta E = |E_{Total}^2 - E_{Total}^1|$) of the system when it is calculated with and without incorporation of the correlation energy term. These results are presented in tables 2 and 3 for two different values of the interaction strength $a_{dd}/a_{ho} = 0.3$ and $a_{dd}/a_{ho} = 1.0$, respectively. From these two tables, we observe that the correlation contribution enhances the stability in the system of 2D dipolar fermions by lowering the total ground-state energy. As expected from equation (11), we find that the contribution of the correlation term is enhanced as the strength of dipolar interaction increases. These results also indicate that the relative percentage difference in the total energy for 10^4 fermions (which is a typical number realized in many experiments with ultracold atoms) is 10.49% and 16.86% for the values of dipolar interaction strength $a_{dd}/a_{ho} = 0.3$ and $a_{dd}/a_{ho} = 1.0$, respectively. Furthermore, from tables 2 and 3, we also observe that the correlation energy exhibits a saturating

Table 3. Same as in table 2, but for dipolar strength of $a_{dd}/a_{ho} = 1.0$.

$a_{dd}/a_{ho} = 1.0$			
N	E_{Total}^1 (woc)	E_{Total}^2 (wc)	$\Delta E/E_{Total}^2$ (%)
100	18.433	16.642	10.76
1000	70.256	61.720	13.83
2500	120.162	104.443	15.05
5000	180.576	155.720	15.96
7500	229.266	196.812	16.49
10000	271.636	232.442	16.86

trend with increasing number of particles. This trend may be attributed to the logarithmic dependence of the correlation energy on the density (see equation (11)). From these results, we conclude that the contribution of the correlation effect significantly lowers the total energy of the system, thereby making it more stable. Therefore, the correlation energy term taking into account the effect of inter-fermion correlation needs to be included for the correct description of a system of 2D dipolar fermions. We also note that the contribution of correlation in ultracold Fermi gas is markedly different from Coulombic systems where the correlation component contribution to the total energy is quite small.

3.2. Collective oscillations

In this section, we discuss the results, highlighting the role of correlation on the frequencies of collective oscillations. To this end, we first briefly describe the sum-rule approach of the many-body linear response theory, which is employed in the present paper for calculating the frequencies of the monopole and quadrupole modes of the collective oscillations. The main advantage of this method is that to calculate the frequencies of

the collective oscillations, it is only necessary to have knowledge of the ground-state wave function or the corresponding density of the system. In the following, we provide a brief description and present the relevant results of the sum-rule approach within linear response theory. For a detailed description of this approach, we refer the reader to some comprehensive reviews already available in the literature [34, 35, 37]. Furthermore, for applications of the sum-rule approach to various 2D systems similar to the one considered in the present paper, we refer the reader to [38–40]. The collective excitations of any system can be investigated by subjecting the system to an external perturbing field. The effect of perturbation is formally included in the Hamiltonian as,

$$H = H_0 + (F e^{i\omega t} + F^\dagger e^{-i\omega t}), \quad (19)$$

where H_0 represents the unperturbed Hamiltonian of the system and F denotes the excitation operator. The choice of this excitation operator is dictated by the nature of the collective mode of excitation. We will come back to the discussion on the choice of the excitation operator F pertinent to our purpose. For a given excitation operator F , the strength function is defined as,

$$S(E) = \sum_n |\langle n|F|0\rangle|^2 \delta(E - E_{n0}), \quad (20)$$

where $|0\rangle$ and $|n\rangle$ are the ground and n th excited states of the unperturbed Hamiltonian H_0 , respectively, and $E_{n0} = E_n - E_0$ represents the excitation energy of the n th excited state. According to the sum-rule approach, it is possible to define various sum rules in terms of the moments of the strength function $S(E)$ given by,

$$\begin{aligned} m_p &= \int E^p S(E) dE \\ &= \sum_n |\langle 0|F|n\rangle|^2 (E_{n0})^p. \end{aligned} \quad (21)$$

For a highly collective excited state, the strength function is almost fully exhausted by this single mode having excitation energy E_{coll} and the corresponding strength function may be approximated as,

$$S(E) = \sigma \delta(E - E_{coll}), \quad (22)$$

where σ is related to the matrix element of F between the ground and the respective collective excited state. Using this approximate expression for $S(E)$, it can be easily verified that,

$$E_{coll} = \sqrt{\frac{m_3}{m_1}}. \quad (23)$$

A more rigorous derivation of the above expression is available in [38, 41]. We note here that for a general case the above expression for E_{coll} represents an upper bound to the energy of a collective excitation. Therefore, to calculate energy/frequency of a collective excitation we need to determine the moments m_3 and m_1 . To this end, we exploit the results that the moments may be expressed as ground-state expectation values of the commutators of the excitation operator F with the unperturbed Hamiltonian H_0 of the many-body system [34, 38]. For example, the moments m_3 and m_1 , which are

relevant to the present study are given by,

$$\begin{aligned} m_1 &= \frac{1}{2} \langle 0|[F^\dagger, [H_0, F]]|0\rangle, \\ m_3 &= \frac{1}{2} \langle 0|[[F^\dagger, H_0], [[H_0, [H_0, F]]]|0\rangle. \end{aligned} \quad (24)$$

To calculate the moments by using the above expressions, we need to specify the excitation operator F for each mode of our interest. Therefore, we now come back to the discussion on the excitation operator F . As mentioned before, the choice of the excitation operator F is dictated by the nature of the collective mode one wants to describe. In this paper, we focus our attention only on the two modes, namely, the breathing or monopole mode and the quadrupole mode. The breathing excitation corresponds to the oscillation of the average radius of the cloud about its ground-state value. In 2D, the breathing or monopole mode is induced by the operator [37, 38],

$$F_m = x^2 + y^2. \quad (25)$$

This operator can be realized by a short switch of the trap frequency. On the other hand, in 2D the multipole excitation operator with polarity l (where $l = 1, 2, \dots$) is given by [38],

$$\begin{aligned} F_l &= (x + iy)^l \\ &= r^l e^{il\theta}. \end{aligned} \quad (26)$$

The excitation operator for the quadrupole mode of collective oscillation corresponds to the case of $l = 2$. The real part of the excitation operator for the quadrupole mode is given by,

$$F_q = x^2 - y^2. \quad (27)$$

Using energy functional for spin-polarized dipolar Fermi gas given by equations (2) to (11) and appropriate scaling transformations of the density given by $\rho_\lambda(\mathbf{r}) \rightarrow \lambda^{1+\alpha} \rho(\lambda x, \lambda^2 y)$, we obtain after some tedious but straightforward algebra, expressions for the frequency of the monopole and quadrupole modes. The basic outline of the derivation of the expressions for frequencies of the two modes is described in appendix B. The expression for the frequency ($\Omega_m = E_{coll}/\hbar$) of the monopole mode is given by (in the unit of harmonic oscillator frequency ω),

$$\begin{aligned} \Omega_m &= \sqrt{2} \left(1 + \frac{U_{TF} + U_{vW}}{U_{ext}} + \frac{9 U_{HF}^1}{4 U_{ext}} \right. \\ &\quad \left. + \frac{9 U_{HF}^2}{4 U_{ext}} + \frac{4 U_c}{U_{ext}} + \frac{I_{c1}}{4 U_{ext}} + \frac{I_{c2}}{4 U_{ext}} \right)^{1/2}, \end{aligned} \quad (28)$$

with

$$\begin{aligned} U_{ext} &= \frac{1}{2} \int r^2 \rho(\mathbf{r}) d\mathbf{r} \\ I_{c1} &= \frac{\hbar^2}{m} \tilde{I}_{c1} \quad \text{and} \quad I_{c2} = \frac{\hbar^2}{m} \tilde{I}_{c2}, \end{aligned} \quad (29)$$

where the expressions for \tilde{I}_{c1} and \tilde{I}_{c2} are given in appendix B. In the above expressions U_{TF} , U_{vW} , U_{HF}^1 , U_{HF}^2 and U_c represent the respective energy functionals calculated with the ground-state density. On the other hand, the expression for the frequency ($\Omega_q = E_{coll}/\hbar$) of the quadrupole mode is given by (in the unit

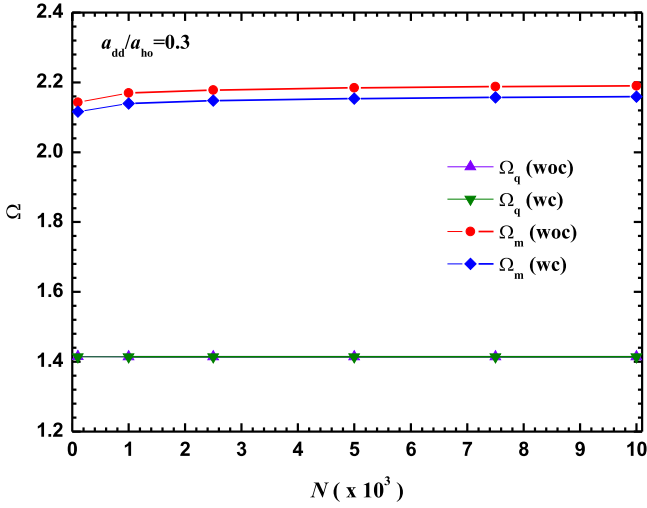


Figure 3. Variation of monopole (Ω_m) and quadrupole (Ω_q) frequencies with number of fermions N for $a_{dd}/a_{ho} = 0.3$. Symbols ‘woc’ and ‘wc’ correspond to ‘without correlation’ effect and ‘with correlation’ effect taken into account, respectively.

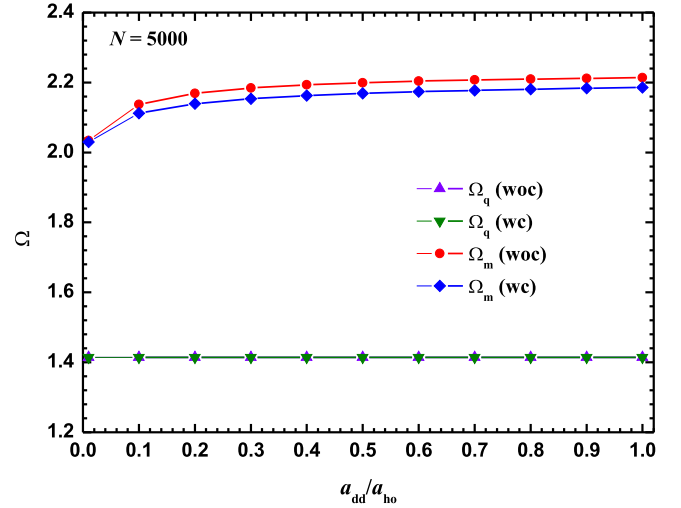


Figure 4. Variation of monopole (Ω_m) and quadrupole (Ω_q) frequencies with dipolar interaction strength a_{dd}/a_{ho} for $N = 5 \times 10^3$ fermions. Symbols ‘woc’ and ‘wc’ correspond to ‘without correlation’ effect and ‘with correlation’ effect taken into account, respectively.

of oscillator frequency ω),

$$\Omega_q = \sqrt{2} \left(1 + \frac{U_{vW}}{U_{ext}} + \frac{J_1}{4U_{ext}} + \frac{J_2}{4U_{ext}} \right)^{1/2}, \quad (30)$$

where

$$J_1 = \frac{\hbar^2}{m} \tilde{J}_1 \quad \text{and} \quad J_2 = \frac{\hbar^2}{m} \tilde{J}_2. \quad (31)$$

The expressions for \tilde{J}_1 and \tilde{J}_2 are given in appendix B. Furthermore, in the process of deriving the above expressions for frequencies, we also obtain virial relation connecting various energy components given by,

$$2U_{TF} + 2U_{vW} - 2U_{ext} + 3U_{HF}^1 + 3U_{HF}^2 + 4U_c + \frac{I_{c1}}{9} = 0. \quad (32)$$

We note that the above expression is a generalization of the virial relation reported in [23], which did not take into account the correlation energy term.

Before presenting the results for the frequencies of collective oscillations, we note that unlike the monopole mode, the expression for the frequency of the quadrupole mode does not explicitly depend on the local TF kinetic, exchange, and correlation energies. Moreover, it can be easily verified that the term J_1 in the expression for Ω_q vanishes for spherically symmetric ground-state density, and like U_{HF}^2 , the magnitude of J_2 is negligibly small for large N . Therefore, we neglect the contribution of J_2 in the expression for Ω_q . In the following, we discuss the results for the frequencies of the monopole and quadrupole modes obtained via equations (28) and (30), respectively, by using the various energy components and the corresponding ground-state densities, which are presented in the last subsection. In figure 3, we display the variation of Ω_m and Ω_q with interaction strength a_{dd}/a_{ho} for $N = 5000$ trapped fermions. On the other hand, in figure 4 we plot Ω_m and Ω_q as functions of the number of trapped fermions N for a

fixed value of $a_{dd}/a_{ho} = 0.3$. First of all, we note that the results presented in figures 3 and 4 match qualitatively with the corresponding results reported in [42], which were obtained without taking into account the inter-particle correlation effect and by employing a method different to the one used in the present paper. Furthermore, we note that the results for the monopole frequency correctly start with $\Omega_m = 2$ for zero interaction and saturate to the value $\Omega_m = \sqrt{5}$ for large value of interaction strength. On the other hand, the values of the quadrupole frequency remain almost constant at $\Omega_q = \sqrt{2}$ throughout the interaction range considered in our work.

Next, we discuss the results, highlighting the role of the correlation part of the particle–particle interaction on the collective oscillations. From figures 3 and 4, we observe that even with the inclusion of the correlation energy term within LDA, the frequency of the quadrupole mode remains more or less fixed at the value of $\sqrt{2}$ and it appears to be independent of both interaction strength and the number of particles on the scale of the plot. From these results, we conclude that the frequency of the quadrupole mode of the collective oscillation is not appreciably altered by the correlation effect (within LDA) over a wide range of values of interaction strength and number of particles. On the other hand, the frequency of the monopole mode is clearly affected by the correlation part of the interaction. In particular, the values of the monopole frequency are lowered due to the inclusion of the correlation energy ($E_c[\rho]$) contribution in the total energy. From figure 3, we observe that the correlation effect leads to nearly uniform (on the scale of plot) lowering of around 1.35% in the magnitude of the monopole frequency in comparison to the case when the correlation effect is not taken into account. Furthermore, from figure 4 it can be seen that the monopole frequency shows similar variation with respect to the increasing number of fermions. The lowering of the

monopole oscillation frequency is consistent with the reduction in the radius of the cloud caused by the attractive nature of correlation potential (discussed in the previous subsection), as the monopole mode excites the oscillation of the radius of the cloud. From the above results, we conclude that the correlation effect not only lowers the ground-state energy of the 2D spin-polarized dipolar fermions, but shifts the monopole frequency of the collective oscillations to lower values.

Before concluding this section, we note here that although the correlation effect introduces a small change in the monopole frequency of the collective oscillations, changes of this order can be detected, as the current experimental development in this area allows one to measure the frequencies of the collective oscillation with very high precision [43]. Therefore, it is expected that the inclusion of the correlation effect in the interaction energy will enhance the match between the theoretical and experimental results for the frequency of the monopole mode of the collective oscillations.

4. Conclusion

In this paper, we have studied the role of the correlation effect on the ground-state properties and on the frequencies of collective oscillations of a spin-polarized dipolar Fermi gas confined in a 2D harmonic trap. We have employed purely the density-based OF-DFT method along with LDA-based expressions for the exchange and correlation energy functionals to calculate the ground-state energies and the density profiles of the dipolar Fermi gases. Using the sum-rule-based approach within linear response theory we have obtained semi-analytical expressions for the frequencies of the monopole and quadrupole modes of the collective oscillations. The calculations of frequencies via these expressions require knowledge of the ground-state densities only. We find that the correlation part of the inter-fermion interaction potential is attractive in nature and it helps in lowering the ground-state energy of a dipolar Fermi gas. The correlation part contributes significantly (around 8%–11%) to the ground-state energy and its contribution increases with increasing values of interaction strength and the number of particles. The attractive nature of the correlation potential is also responsible for reduction in the size and enhancement of the peak density of the trapped fermionic cloud. Similarly, we find that the reduction in the radius of the cloud due to the correlation effects also lowers the frequency of the monopole mode of the collective oscillations appreciably in comparison to the cases for which the correlation part of the interaction is neglected. In contrast to this, the inclusion of the correlation part within LDA in the interaction energy and potential does not alter the frequency of the quadrupole mode of the collective oscillation appreciably for a wide range of values of interaction strength and the number of fermions contained in the trap.

Appendix A

In this appendix, we give a brief description of the method employed to solve equation (18), which is a nonlinear Kohn–Sham-like equation in a self-consistent manner. First, we rewrite equation (18) by scaling the coordinates and energy with harmonic oscillator length ($a_{ho} = \sqrt{\hbar/m\omega}$) and oscillator energy ($\hbar\omega$), respectively. Next, we consider the corresponding time-dependent counterpart of equation (18) and then change time t by $\tau = -it$, which leads to,

$$\frac{\partial \phi(r)}{\partial \tau} = -H(\tau)\phi(r), \quad (\text{A1})$$

where Hamiltonian H is,

$$H(\tau) = -\frac{1}{2}\nabla^2 + v'_{eff}(r, \tau). \quad (\text{A2})$$

The formal solution of equation (A1) can be written as,

$$\phi(r, \tau + \Delta\tau) = e^{-\Delta\tau \hat{H}(\tau)} \phi(r, \tau), \quad (\text{A3})$$

with $\Delta\tau \ll 1$.

The function $\phi(r)$ is evolved in time by $\Delta\tau$ via a non-unitary exponential operator $e^{-\hat{H}\Delta\tau}$ iteratively. After sufficiently long time evolution (i.e. large τ limit) the ground-state wave function is retrieved as the higher excited states decay much faster compared to the ground state.

To proceed further, we choose polar coordinate system (r, θ) , and the Hamiltonian operator in this coordinate system can be written as,

$$\hat{H} = -\frac{1}{2}\frac{\partial^2}{\partial r^2} - \frac{1}{2r}\frac{\partial}{\partial r} - \frac{1}{2r^2}\frac{\partial^2}{\partial \theta^2} + v'_{eff}. \quad (\text{A4})$$

For the ground state, the third term in the above equation (equation (A4)) vanishes as the ground-state density is independent of θ . Thus, equation (A1) transforms into a 1D differential equation surviving in variable r . This variable can be discretized as $r_j = jh$ with integer $j = 1, 2, \dots, M$. In our calculations, we have used $h = 0.008$. After discretization, equation (A3) can be rewritten in more symmetric form as,

$$e^{\frac{\Delta\tau}{2}\hat{H}_j}\phi_j^{n+1} = e^{-\frac{\Delta\tau}{2}\hat{H}_j}\phi_j^n, \quad (\text{A5})$$

where superscript n corresponds to time discretization. The expansion of the exponential operator on both sides up to first order and approximating the operators $\partial/\partial r$ and $\partial^2/\partial r^2$ by two- and three-point difference formulae yield the following set of M simultaneously equations:

$$P_j\phi_{j-i}^{n+1} + Q_j\phi_j^{n+1} + R_j\phi_{j+1}^{n+1} = S_j^n, \quad (\text{A6})$$

where

$$P_j = -\frac{\Delta\tau}{4h^2} + \frac{\Delta\tau}{8r_j h}, \quad Q_j = 1 + \frac{\Delta\tau}{2h^2} + \frac{\Delta\tau}{2}v'_{eff},$$

$$R_j = -\frac{\Delta\tau}{4h^2} - \frac{\Delta\tau}{8r_j h}, \quad (\text{A7})$$

$$S_j^n = -P_j\phi_{j-1}^n + T_j\phi_j^n - R_j\phi_{j+1}^n,$$

$$T_j = 1 - \frac{\Delta\tau}{2h^2} - \frac{\Delta\tau}{2}v'_{eff}. \quad (\text{A8})$$

Furthermore, equation (A6) can be written in the form of a tri-diagonal matrix equation:

$$\begin{bmatrix} Q_1 & R_1 & & & 0 \\ P_2 & Q_2 & R_2 & & \\ & P_3 & Q_3 & \ddots & \\ & & & \ddots & R_{M-1} \\ 0 & & P_M & Q_M & \end{bmatrix} \begin{bmatrix} \phi_1^{n+1} \\ \phi_2^{n+1} \\ \vdots \\ \phi_{M-1}^{n+1} \\ \phi_M^{n+1} \end{bmatrix} = \begin{bmatrix} S_1^n \\ S_2^n \\ \vdots \\ S_{M-1}^n \\ S_M^n \end{bmatrix}.$$

To solve equation (A6) self-consistently, we start with an initial guess of the wave function ϕ_j^n to obtain for ϕ_j^{n+1} by Thomas algorithm [44]. In this scheme, the parameter $\Delta\tau$ needs to be chosen carefully so that the truncation of exponential beyond first order in $\Delta\tau$ remains valid. In the present work, we have chosen $\Delta\tau = 10^{-5}$ for our calculations. Ground-state wave function should satisfy both cusp and asymptotic conditions. Therefore, $\frac{1}{2r} \frac{\partial \phi}{\partial r}$ has to be zero at $r = 0$, so $\phi_0^n = \phi_1^n$ (ϕ_0^n is wave function at $r = 0$) and the wave function is required to vanish at the end point of the mesh. After solving for ϕ_j^{n+1} , we update H with generated ϕ_j^{n+1} , which is properly normalized to N . The convergence criterion for achieving the self-consistent solution is taken to be $\sum_j^M |\phi_j^{n+1} - \phi_j^n| < \epsilon$. The ground-state energy can be calculated by substituting the converged density into equation (2).

Appendix B

In this appendix, we give an outline of the basic steps involved in the derivation of the expressions for moments m_1 and m_3 , and which in turn yield the frequency of the collective oscillations via equation (23). To this end, we first combine the excitation operators for the monopole and quadrupole modes and construct a general operator given by,

$$F = x^2 + \alpha y^2, \tag{B1}$$

with $\alpha = 1$ and $\alpha = -1$ representing the monopole and quadrupole modes, respectively.

Using the above expression for F and the commutator relations $[x, p_x] = [y, p_y] = i\hbar$, it can be shown that,

$$\begin{aligned} m_1 &= \frac{1}{2} \langle 0 | [F^\dagger, [H_0, F]] | 0 \rangle, \\ &= \frac{2\hbar^2}{m} \langle 0 | x^2 + \alpha^2 y^2 | 0 \rangle. \end{aligned} \tag{B2}$$

Therefore, for both the monopole and quadrupole modes, the above expression for the first moment m_1 can be written as,

$$m_1 = \frac{2\hbar^2}{m} \int r^2 \rho(\mathbf{r}) d\mathbf{r}. \tag{B3}$$

The calculation of the third moment m_3 is more involved and it can be calculated by employing appropriate scaling transformation of the ground-state wave function [34, 38]. For this purpose, we define a transformed ground-state wave function as,

$$|\Phi_\eta\rangle = e^{\eta Q} |0\rangle, \tag{B4}$$

where Q is an anti-Hermitian operator given by $Q = [H_0, F]$. Furthermore, it can be shown that the spatial form of the transformed wave function can be written as,

$$\Phi_\eta(x, y) = \lambda^{(1+\alpha)/2} \Phi_0(\lambda x, \lambda^\alpha y), \tag{B5}$$

where $\lambda = e^{-\frac{2\hbar^2}{m}\eta}$. In terms of scaled wave function $|\Phi_\eta\rangle$, the third moment m_3 can be written as,

$$m_3 = \frac{1}{2} \frac{\partial^2}{\partial \eta^2} \langle \Phi_\eta | H_0 | \Phi_\eta \rangle |_{\eta=0}. \tag{B6}$$

Now, the Hohenberg–Kohn theorem of DFT allows us to write $\langle \Phi_\eta | H_0 | \Phi_\eta \rangle = E[\rho_\eta]$ with,

$$E[\rho_\eta] = T_s[\rho_\eta] + E_{ext}[\rho_\eta] + E_{int}[\rho_\eta], \tag{B7}$$

where $E_{ext}[\rho_\eta] = \int v_{ext}(\mathbf{r}) \rho_\eta(\mathbf{r}) d\mathbf{r}$ and the transformed density ρ_η is given by,

$$\rho_\eta(x, y) = \lambda^{1+\alpha} \rho(\lambda x, \lambda^\alpha y). \tag{B8}$$

Now, by combining equations (B6) and (B7) we get the following expression for the third moment m_3 :

$$m_3 = m_3(T_s) + m_3(E_{ext}) + m_3(E_{int}), \tag{B9}$$

where

$$\begin{aligned} m_3(T_s) &= \frac{1}{2} \frac{\partial^2}{\partial \eta^2} T_s[\rho_\eta] |_{\eta=0} \\ m_3(E_{ext}) &= \frac{1}{2} \frac{\partial^2}{\partial \eta^2} E_{ext}[\rho_\eta] |_{\eta=0} \\ m_3(E_{int}) &= \frac{1}{2} \frac{\partial^2}{\partial \eta^2} E_{int}[\rho_\eta] |_{\eta=0}. \end{aligned} \tag{B10}$$

Finally, by using the above relations and the forms for various energy components given by equations (2) to (11), we arrive at the following expressions for the respective contributions to m_3 :

$$m_3(T_s) = \frac{1}{2} \left(\frac{2\hbar^2}{m} \right)^2 [(1 + \alpha)^2 T_{TF}[\rho] + 4T_{vW}[\rho]], \tag{B11}$$

$$m_3(E_{ext}) = \frac{1}{2} \left(\frac{2\hbar^2}{m} \right)^2 4E_{ext}[\rho], \tag{B12}$$

$$m_3(E_{HF}^1) = \frac{1}{2} \left(\frac{2\hbar^2}{m} \right)^2 \frac{9}{4} (1 + \alpha)^2 E_{HF}^1[\rho]. \tag{B13}$$

The calculation of the contribution of E_{HF}^2 to m_3 is more involved and requires some lengthy algebra. We get the following expressions for $m_3(E_{HF}^2)$: for the case of $\alpha = 1$

$$m_3(E_{HF}^2) = \frac{1}{2} \left(\frac{2\hbar^2}{m} \right)^2 9E_{HF}^2[\rho], \tag{B14}$$

and on the other hand, for $\alpha = -1$

$$m_3(E_{HF}^2) = \frac{1}{2} \left(\frac{2\hbar^2}{m} \right)^2 (\tilde{J}_1 + \tilde{J}_2), \quad (\text{B15})$$

where

$$\begin{aligned} \tilde{J}_1 &= -\pi a_{dd} \int \rho(\mathbf{r}) d\mathbf{r} \int d\mathbf{r}' \int \frac{d\mathbf{k}}{(2\pi)^2} F_1(\mathbf{k}) e^{-i\mathbf{k}\cdot(\mathbf{r}-\mathbf{r}')} \rho(\mathbf{r}') \\ \tilde{J}_2 &= -\pi a_{dd} \int \rho(\mathbf{r}) d\mathbf{r} \int d\mathbf{r}' \int \frac{d\mathbf{k}}{(2\pi)^2} F_2(\mathbf{k}) e^{-i\mathbf{k}\cdot(\mathbf{r}-\mathbf{r}')} \rho(\mathbf{r}'), \end{aligned} \quad (\text{B16})$$

with

$$\begin{aligned} F_1(\mathbf{k}) &= \frac{k_x^2 - k_y^2}{(k_x^2 + k_y^2)^{1/2}} \\ F_2(\mathbf{k}) &= \frac{2k_y^2(3k_x^2 + k_y^2)}{(k_x^2 + k_y^2)^{3/2}}. \end{aligned} \quad (\text{B17})$$

Similarly, after some tedious algebra we get the following expressions for the contribution of $E_c[\rho]$ to m_3 :

$$m_3(E_c) = \frac{1}{2} \left(\frac{2\hbar^2}{m} \right)^2 (16E_c[\rho] + \tilde{I}_{c1} + \tilde{I}_{c2}), \quad (\text{B18})$$

where

$$\begin{aligned} \tilde{I}_{c1} &= 18\pi^2 a_{dd}^2 \int \rho^3(\mathbf{r}) \left[\frac{Y(\mathbf{r})}{X(\mathbf{r})(1+X(\mathbf{r}))} \right] d\mathbf{r} \\ \tilde{I}_{c2} &= -2\pi^2 a_{dd}^2 \int \rho^3(\mathbf{r}) \\ &\times \left[\frac{(Y^2(\mathbf{r}) + 2Y(\mathbf{r})X(\mathbf{r}) - X(\mathbf{r})Z(\mathbf{r}) - X^2(\mathbf{r})Z(\mathbf{r}))}{X^2(\mathbf{r})(1+X(\mathbf{r}))^2} \right] d\mathbf{r}, \end{aligned} \quad (\text{B19})$$

with

$$\begin{aligned} X(\mathbf{r}) &= A\rho^{1/4}(\mathbf{r}) + B\rho^{1/2}(\mathbf{r}) + C\rho^{3/4}(\mathbf{r}) \\ Y(\mathbf{r}) &= \frac{A}{2}\rho^{1/4}(\mathbf{r}) + B\rho^{1/2}(\mathbf{r}) + \frac{3C}{2}\rho^{3/4}(\mathbf{r}) \\ Z(\mathbf{r}) &= -\frac{A}{4}\rho^{1/4}(\mathbf{r}) + \frac{3C}{4}\rho^{3/4}(\mathbf{r}), \end{aligned} \quad (\text{B20})$$

for $\alpha = 1$ and

$$m_3(E_c) = 0, \quad (\text{B21})$$

for $\alpha = -1$. We use the above expressions for the contribution of various energy components to m_3 and m_1 to calculate the frequencies of the monopole and quadrupole modes of the collective oscillations.

ORCID iDs

Rashmi Gangwar  <https://orcid.org/0000-0002-9422-2987>

References

[1] Baranov M 2008 *Phys. Rep.* **464** 71
 [2] Ospelkaus S, Ni K-K, de Miranda M H G, Neyenhuis B, Wang D, Kotochigova S, Julienne P S, Jin D S and Ye J 2009 *Faraday Discuss.* **142** 351
 [3] Ni K-K, Ospelkaus S, Wang D, Quemener G, Neyenhuis B, de Miranda M H G, Bohn J L, Ye J and Jin D S 2010 *Nature* **464** 1324

[4] Ospelkaus S, Ni K-K, Wang D, de Miranda M H G, Neyenhuis B, Quémener G, Julienne P S, Bohn J L, Jin D S and Ye J 2010 *Science* **327** 853
 [5] Park J W, Will S A and Zwierlein M W 2015 *Phys. Rev. Lett.* **114** 205302
 [6] de Miranda M H G *et al* 2011 *Nat. Phys.* **7** 502
 [7] De Marco L, Valtolina G, Matsuda K, Tobias W G, Covey J P and Ye J 2019 *Science* **363** 853–6
 [8] Baranov M A, Mar'enko M S, Rychkov V S and Shlyapnikov G V 2002 *Phys. Rev. A* **66** 013606
 [9] Cooper N R and Shlyapnikov G V 2009 *Phys. Rev. Lett.* **103** 155302
 [10] Levinsen J, Cooper N R and Shlyapnikov G V 2011 *Phys. Rev. A* **84** 013603
 [11] Pikovski A, Klawunn M, Shlyapnikov G V and Santos L 2010 *Phys. Rev. Lett.* **105** 215302
 [12] Baranov M A, Micheli A, Ronen S and Zoller P 2011 *Phys. Rev. A* **83** 043602
 [13] Sieberer L M and Baranov M A 2011 *Phys. Rev. A* **84** 063633
 [14] Modugno G, Ferlaino F, Heidemann R, Roati G and Inguscio M 2003 *Phys. Rev. A* **68** 011601(R)
 [15] Jochim S, Bartenstein M, Altmeyer A, Hendl G, Chin C, Denschlag J H and Grimm R 2003 *Phys. Rev. Lett.* **91** 240402
 [16] Günter K, Stöferle T, Moritz H, Köhl M and Esslinger T 2005 *Phys. Rev. Lett.* **95** 230401
 [17] Martiyanov K, Makhalov V and Turlapov A 2010 *Phys. Rev. Lett.* **105** 030404
 [18] Dyke P, Kuhnle E D, Whitlock S, Hu H, Mark M, Hoinka S, Lingham M, Hannaford P and Vale C J 2011 *Phys. Rev. Lett.* **106** 105304
 [19] van Zyl B P, Kirkby W and Ferguson W 2015 *Phys. Rev. A* **92** 023614
 [20] Block J K and Bruun G M 2014 *Phys. Rev. B* **90** 155102
 [21] Parish M M and Marchetti F M 2012 *Phys. Rev. Lett.* **108** 145304
 [22] Sun K, Wu C and Das Sarma S 2010 *Phys. Rev. B* **82** 075105
 [23] Fang B and Englert B-G 2011 *Phys. Rev. A* **83** 052517
 [24] van Zyl B P, Zaremba E and Pisarski P 2013 *Phys. Rev. A* **87** 043614
 [25] Abedinpour S H, Asgari R, Tanatar B and Polini M 2014 *Ann. Phys. (NY)* **340** 25
 [26] Ustunel H, Abedinpour S H and Tanatar B 2014 *J. Phys.: Conf. Ser.* **568** 012020
 [27] Matveeva N and Giorgini S 2012 *Phys. Rev. Lett.* **109** 200401
 [28] Lu Z K and Shlyapnikov G V 2012 *Phys. Rev. A* **85** 023614
 [29] Ancilotto F 2015 *Phys. Rev. A* **92** 061602(R)
 [30] Parr R G and Yang W 1999 *Density Functional Theory of Atoms and Molecules* (Oxford: Oxford University Press)
 [31] Perdew J P and Kurth S 2003 *A Primer in Density Functional Theory* ed C Fiolhais, F Nogueira and M Marques (Berlin: Springer)
 [32] Driezler R M and Gross E K U 1990 *Density Functional Theory: An Approach to the Quantum Many-Body Problem* (Berlin: Springer)
 [33] Das A K and Banerjee A 2018 *Eur. Phys. J. D* **72** 111
 [34] Bohigas O, Lane A M and Martorell J 1979 *Phys. Rep.* **51** 267
 [35] Lipparini E and Stringari S 1989 *Phys. Rep.* **175** 103
 [36] Dey B K and Deb B M 1999 *J. Chem. Phys.* **110** 13
 [37] Abraham J W and Bonitz M 2014 *Contrib. Plasma Phys.* **54** 27
 [38] Sinha S 1997 *Phys. Rep. A* **55** 4325
 [39] Banerjee A 2004 *Phys. Lett. A* **332** 291
 [40] Banerjee A and Tanatar B 2005 *Phys. Rev. A* **72** 053260
 [41] Lipparini E, Barberan N, Barranco M, Pi M and Serra L 1997 *Phys. Rev. B* **56** 12375
 [42] van Zyl B P, Zaremba E and Towers J 2014 *Phys. Rev. A* **90** 043621
 [43] Wu Y-P *et al* 2018 *Phys. Rev. B* **97** 020506(R)
 [44] Smith G D 1965 *Numerical Solution of Partial Differential Equations* (Oxford: Oxford University Press)